INFLUENCE OF FIBER PACKING STRUCTURE ON PERMEABILITY

Zhong Cai
Drexel University
Philadelphia, PA 19104

Alexander L. Berdichevsky
CR Industries
Elgin, IL 60123

ABSTRACT

The study on the permeability of an aligned fiber bundle is the key building block in modeling the permeability of advanced woven and braided preforms. Available results on the permeability of fiber bundles in the literature show that substantial difference exists between numerical and analytical calculations on idealized fiber packing structures, such as square and hexagonal packing, and experimental measurements on practical fiber bundles. The present study focuses on the variation of the permeability of a fiber bundle under practical process conditions. Fiber bundles are considered as containing openings and fiber clusters within the bundle. Numerical simulations on the influence of various openings on the permeability have been conducted. Idealized packing structures are used, but with introduced openings distributed in different patterns. Both longitudinal and transverse flow are considered. The results show that openings within the fiber bundle have substantial effect on the permeability. In the longitudinal flow case, the openings become the dominant flow path. In the transverse flow case, the fiber clusters reduce the gap sizes among fibers. Therefore the permeability is greatly influenced by these openings and clusters respectively. In addition to the porosity or fiber volume fraction, which is commonly used in the permeability expression, another fiber bundle status parameter, the ultimate fiber volume fraction, is introduced to capture the disturbance within a fiber bundle.

INTRODUCTION

The permeability of an aligned fiber bundle has been studied extensively since it is an important parameter in the composite manufacturing processes. Different proposed formulas have been suggested and verified by experiments for both longitudinal and transverse permeabilities [1-6]. It was found that the permeability is closely related to the fiber volume fraction or porosity. However, experimental measurements showed large scattering of data. Numerical calculations of the permeability of idealized square and hexagonal packing structures are also reported [7, 8].

The permeability is defined as [9]

$$K = \frac{Q}{A}\frac{\mu}{(\Delta p/L)} \qquad (1)$$

Presented at FIBER-TEX'92, Philadelphia, October, 1992.

where Q is the volume flow rate, A is the total cross-section area, and μ is the viscosity. The pressure difference Δp is across the distance L. Here the positive values of Q and Δp are used although their directions are opposite. In order to use the dimensionless parameter, the permeability K is normalized by using the fiber radius r_f. The normalized permeability K* is defined as

$$K^* = \frac{K}{r_f^2} \tag{2}$$

When permeability in different directions is discussed, subscript x is used for the fiber direction, and y and z refer to transverse directions. Since a fiber bundle is assumed to be transversely isotropic, only subscript z is used to express the transverse permeability.

The comparison of the permeability of these idealized packing structures and other proposed formulas is summarized in Fig. 1 for both longitudinal and transverse cases. In the longitudinal direction, there is a substantial difference between the model predictions, which are backed by experimental data, and numerical solutions. The disturbance in the fiber bundle under the processing conditions contributes to the discrepancy. In the transverse direction, two models are used in the comparison. Kardos' model [3, 4] only contains fiber volume fraction V_f, while Gutowski's model [2] introduced an additional variable, the ultimate fiber volume fraction V_a. There are some differences between Kardos' model and square packing results, and between Gutowski's model and hexagonal packing results respectively. The difference between these two groups becomes substantial when V_f becomes high.

As a fiber bundle usually contains thousands of filaments, the random distribution of these filaments, and any disturbance within a bundle, can result in the change of permeability of the fiber assembly. In this study, micro-level cell models with introduced disturbance are built to investigate these disturbances using numerical simulations. The variation of the permeability due to these disturbances is then assessed and analyzed.

NUMERICAL SIMULATION

The numerical simulation work was done by using the available finite element packages ANSYS [10] and FIDAP [11]. The automatic meshing capability and the easiness of the pre-processing and post-processing of these FE packages especially with ANSYS greatly help build up various mesh models.

a) Longitudinal Permeability

For the longitudinal permeability, we assume the flow is parallel to the fiber axis, or x direction, and only the velocity component V_x exists. Also we assume the Reynolds number is very small and the gravity can be neglected so that this becomes the so-called Stokes flow. The flow equation can be written as

$$\frac{\partial p}{\partial x}\frac{1}{\mu} = \frac{\partial^2 V_x}{\partial y^2} + \frac{\partial^2 V_x}{\partial z^2} \tag{3}$$

where the terms at the left side are constant over the whole y-z plane. This is equivalent to a 2-D thermal equation with a uniform heat generation over the whole region which can be expressed as

$$\frac{w}{k} = \frac{\partial^2 T}{\partial y^2} + \frac{\partial^2 T}{\partial z^2} \qquad (4)$$

When this heat transfer equation is solved, the temperature distribution obtained is equivalent to the velocity field for the flow equation. The longitudinal permeability can be solved accordingly.

2-D thermal elements are used in the calculation. This is a four-node plane element with a single degree of freedom, temperature, at each node. The reference temperature is set as zero at the fiber surface. Therefore the values of the temperature are directly used as the relative magnitude of the temperature rise.

The computational cell is set as a rectangle of L_y by L_z in y and z directions respectively. Symmetry boundary conditions are set at four cell boundaries, y=0, y=L_y, z=0, and z=L_z.

b) Transverse Permeability

For the transverse flow with small Reynolds number, the Stokes equation becomes

$$\frac{1}{\mu}\frac{\partial p}{\partial y} = \nabla^2 V_y$$

$$\frac{1}{\mu}\frac{\partial p}{\partial z} = \nabla^2 V_z$$

$$\nabla^2 = \frac{\partial^2}{\partial y^2} + \frac{\partial^2}{\partial z^2} \qquad (5)$$

The permeability K is calculated directly from the averaged flow rate according to the definition.

The 2-D 4-node fluid element is used in the simulation. In the calculation the option is set as steady state flow, and the constants for the body force are set to be zero. Also the local Reynolds number for the elements is set to be much smaller than 1. The boundary conditions set on the representative cell (L_y by L_z) are: 1) at the surfaces of z=0 and z=L_z, V_z=0 and $\partial V_y/\partial z$=0; 2) at the surfaces of y=0 and y=L_y, V_z=0 and $\partial V_y/\partial y$=0; and 3) the pressure difference $(p)_{y=0} - (p)_{y=L} = \Delta p$. Along the surfaces of y=0 and y=L_y, the pressure is also constant.

DENSELY PACKED HOLLOW STRUCTURES

Numerical simulations on hollow hexagonal packing and hollow square packing are reported in [8]. These hollow packing structures possess relatively low ultimate fiber volume fraction, 0.589 for hollow square packing and 0.605 for hollow hexagonal packing. The experimental data of the ultimate fiber volume fraction for an aligned fiber bundle was in the range of 0.78 to 0.85 [2]. In this part of the numerical simulation, hexagonal and square packing structures are still used, with a portion of the fibers removed in a certain pattern. They become densely packed hollow structures. In other words, the

densely packed fibers are assumed to have sparsely distributed voids in the bundle. However, since they are densely packed, there are always "good" lock mechanisms. In other words, these voids are not connected to each other and there is no direct flow path within the bundle.

Since there are different amounts of the fibers removed in different mesh models, the ultimate fiber volume fraction V_a will be different for each of the options. Therefore this simulation reveals more the effect of V_a on the permeability variations.

The computation cells are chosen to be rectangular, so that mirror symmetric boundary conditions can be set at each side. The hollow packing settings are also constructed such that the isotropic behavior of the permeability is always preserved.

Different computational cells are shown in Figs. 2 and 3. Finite element meshes of these computational cells are also shown in these figures. The convergence of the calculations is checked by comparing the results with available "exact" solutions for hexagonal and square packing, and by varying mesh size and increasing element and node numbers. The convergence of the calculation for other structures is also checked on selected samples. Fig. 4 shows the convergence of the calculation versus element number for the mixed packing structure. When determining the mesh size, a compromise is reached by considering both the accuracy and the computational time.

QUASI-RANDOM PACKING MODEL

In studying the transverse stiffness of the unidirectional composites, Adams and Tsai [12] proposed a numerical method which used a random array of cells to represent the micro-level composite structure. We adopt the same approach and build a random set of cells to represent the micro-level fiber assembly with some random disturbance. In other words, the fiber assembly contains closely packed fibers and some open spaces among fibers, which are randomly placed into cells.

The representative volume contains twenty-five unit cells (5 by 5). It is a quarter of the representative volume of 10 by 10, as shown in Fig. 5. Mirror symmetry boundary conditions are imposed on the 5 by 5 cell to reduce the amount of the calculation. It is also assumed that the cell retains the isotropic permeability, which means the permeabilities in the y and z directions are the same. This is realized by the symmetry condition imposed on the +45 degree diagonal.

Two random effects are investigated. One is the random packing pattern, which means some of the cells are filled with fibers while others are empty. The other is the random positioning of fibers within the cell "box", which means fibers are placed at the off-center locations in cells.

The random function in the FORTRAN program language is used to generate the random cell packing and the random center positions. The random function generator in the program is controlled by the seed number. In order to obtain the randomness of the seed number, the time function was used which was related to the time to the one hundredth of a second. The random number obtained from the time function was then transformed into a series of random seed numbers. For each random fiber packing, 15 random numbers were assigned to 25 cells under the rule of symmetry to the diagonal. These cells were ranked according to the magnitude of the random number. Then the lowest N cells were chosen as filled with fibers, where N was determined according to the fiber volume fraction and fiber radius. This program was named as RAND-F. For the random center positions, 15 random numbers were transformed to a value between $-\delta$ and $+\delta$ respectively, where δ was

the maximum offset of the fiber center position determined by the cell mesh condition and the fiber radius. This program was named as RAND-D.

Automatic meshing was used to generate different random packing models. As mentioned earlier, three sets of random packings were tried. The first was the random occupancy of fiber cells, the second was the fully occupied fiber cells with random offset fiber center positions, and the third was the combination of these two, which meant only some cells were randomly filled with fibers which were located at random off-center positions.

For the random occupancy of fiber cells, two basic unit cells were setup to represent the cells with and without fibers, as shown in Fig. 5. The packing pattern generated from the RAND-F program was used as the input, and indices 1 and 0 were assigned to corresponding cells. 25 local coordinate systems were used for these cells and they were located at the center of these cells. Meshing was done for each cell according to the given index (1: with fiber; 0: without fiber). Finally these meshed cells were combined together, repeated nodes were merged, and boundary conditions were set accordingly.

For the random offset position of fiber centers, the fiber center positions were first determined by the RAND-D program. These positions were used to generate the fiber boundaries within the cell. The original cell center positions were used to generate cell boundaries. Then the meshes were automatically generated. Because the offset of the fiber centers sometimes introduced difficulty in automatic meshing, errors did occur and the pre-processing was aborted. Due to the limitation of the automatic meshing used, fibers were always contained in the original cells, which greatly limited the extent of the variation on the permeability.

For the third situation of random fiber cells and random fiber center positions, both programs (RAND-F and RAND-D) were used and automatic meshing was applied accordingly.

The computational error is directly related to the mesh size. This was checked for a particular case by varying the mesh size. As a compromise of the accuracy and the computational time, the mesh model chosen contained 144 elements (12 by 12) for cells without fibers, and 240 or 288 elements (48 in the circumferential direction and 5 or 6 in the radial direction) for cells with fibers. The estimated error in the worst case was less than 1 percent, and in most other cases, the error was around 0.2 to 0.5 percent.

RESULTS AND DISCUSSIONS

The permeability results of the densely packed fibers with introduced openings are shown in Fig. 6 and 7 for longitudinal and transverse directions respectively. These structures have definite packing patterns. All the gaps among fibers are with the same width. All the openings introduced are isolated. Therefore, if we keep squeezing these fiber bundles, the values of V_a will be different in each case. It is shown in the figures that with relatively high fiber volume fraction, the effect of V_a on the permeability increases.

As we mentioned earlier, the effect of the openings on the permeability is different in different flow directions. In the longitudinal flow case, the openings provide the flow path to the fluid. In the transverse flow case, the openings reduce the gap width among fibers, resulting in higher flow resistance. In Fig. 6, the three cases without introduced openings, hexagonal, square, and mixed packings, show relatively low longitudinal permeability.

The variation of the permeability due to different packing is substantial. In the longitudinal direction, at the V_f=0.5, the permeability can be about 2.7 times of difference, while in the

transverse direction, the difference can be about 10 times. Therefore, with only one variable, usually the fiber volume fraction V_f, the permeability status of the fiber bundle is possibly still very uncertain.

Fig. 8 shows the permeability variation of random packing structures. As shown in Fig. 5, there are three groups of packing situations with the randomly placed fiber cells. We define them as with fiber locking, without fiber locking, and with direct flow path. In the case of with fiber locking, there exists a row of fibers or a combination of rows of fibers to lock the flow if the maximum packing efficiency of that particular packing is reached. In other words, fluid has to pass through small gaps within the fiber row. In the case of without fiber locking, which means that even at the maximum packing efficiency flow is still possible, the relatively large gaps in the diagonal direction of the cell provide easier flow path for the fluid. In other words, flow paths are mainly in the diagonal directions. In the case of with direct flow path, there exists a row or a combination of rows of open spaces as the flow path.

For each of the selected fiber volume fractions, there are options of number of fiber cells. The percentage of the occurrence of each of these three cases depends on the fiber cell numbers. With 14 fiber cells out of the 25 total cells, there were a few cases of direct flow path, and the rest were with fiber locking or without fiber locking. With 16 fiber cells, the occurrence of direct flow path diminished so that there were mainly cases of with fiber locking and without fiber locking. With 18 or more fiber cells, most of the cases were with the locking of fibers.

The number of cells with fibers is also limited by the fiber volume fraction. With relatively low fiber volume fraction, less fiber cell numbers are possible. For example, for V_f=0.4, we tried fiber cell numbers of 14, 16, 18, and 20. For V_f=0.45, fiber cell numbers were 16, 18, and 20. For V_f=0.5, fiber cell numbers were 17 and 19.

The simulation of the randomly packed fibers was done on these three groups. With 14 to 20 fiber cells, the simulation covers V_f range of 0.2 to 0.5. With 25 fiber cells but random center positions, the range of V_f was from 0.2 to 0.7. With 18 to 20 fiber cells and offset fiber center positions, the range of V_f was 0.4 to 0.55. For each selected case, 25 simulations were performed with different random settings. However, because of the automatic mesh limitation, only meshes with "good" shape were accepted for the finite element calculation. Therefore the successful simulations for each case were usually less than 25. The total simulation cases were over 700 for longitudinal and transverse flow respectively.

Fig. 8a shows the data variation of the permeability when different numbers of the fiber cells are used in the simulation. With each selected fiber cell number, there are about 20 data points. The variations are very substantial. In the longitudinal case, the difference is as high as more than five times. In the transverse direction, the difference can be as high as over a hundred times.

Hexagonal packing is used as a reference in Fig. 8a. In the longitudinal flow case, it is a low limit of the permeability, since it possesses the most uniformly distributed flow channels. In the transverse flow case, however, there were cases that the permeability is higher or lower than that of the hexagonal packing. In the extreme cases, fibers may fully lock the flow path when they contact with each other, or they may be far away from each other so that a large flow path with minimum flow resistance may form within the bundle.

In Fig. 8a about the transverse permeability, three groups of data can be distinguished. In the 14 fiber cell case, the group with locked fibers shows the normalized permeability of

about 0.001, the group without fiber locking shows the normalized permeability of about 0.04, and the group with direct flow path shows the normalized permeability of about 0.2. With 16 fiber cells, only two groups appear, with fiber locking and without fiber locking. The permeability values are about 0.08 and 0.04 respectively. With 18 or more fiber cells, only locked fiber cells exist. Also with the increase of the fiber cells, the permeability data of locked fibers gradually gets close to that of the hexagonal packing.

Fig. 8b shows the variation of the permeability when all 25 cells are filled with fibers, but the fiber center positions are randomly determined. The variation of the permeability in both longitudinal and transverse cases is substantially smaller than that in Fig. 8a. It is also interesting to see that in the longitudinal case, the permeability of these random fiber sets is always higher than that of the original square packing. In the transverse case, however, the variation appears in both directions, resulting in either higher or lower permeability values. This agrees with the results shown in Fig. 1, where the longitudinal permeability data from experiments is substantially higher than that of the idealized packing, and the transverse permeability data from experiments is more close to that of the idealized packing.

For a real fiber bundle under the processing conditions, the macro-level status of the fiber bundle is already determined. In other words, the relative positions of the fibers within the bundle are somewhat settled. Gently squeezing the fiber bundle will not change the macro-level status of the bundle. With this relatively determined fiber bundle status, the variation of the permeability for a certain fiber bundle is limited. However, different fiber bundles may have substantially different status, such as opening size within the bundle. Therefore the permeability from bundle to bundle may be very different. To capture this macro-level fiber bundle status, additional status variables are needed. In [2] and [7], the ultimate fiber volume fraction is introduced in addition to the average fiber volume fraction. More discussions and proposed models on selecting the ultimate fiber volume fraction as the additional permeability parameter are presented in [13].

SUMMARY

Finite element simulations on the variation of the permeability of an aligned fiber bundle have been carried out. These simulations are based on the idealized packing with introduced openings, and based on the quasi-random fiber cell models. The results show that even with the same fiber volume fraction, the permeability variation can vary substantially. The disturbance within a fiber bundle has to be considered in order to reduce the uncertainty in the estimation about the permeability.

The numerical simulation results also suggest that in addition to the average fiber volume fraction, other parameters describing the macro-level status of a fiber bundle are needed. The effect of the ultimate fiber volume fraction on the permeability is investigated through the simulation.

ACKNOWLEDGEMENTS

The authors would like to thank D.J. Lawrie for many helpful discussions and technical supports during the course of this work.

REFERENCES

1. Williams, J.G., Morris, C.E.M., and Ennis, B.C., "Liquid Flow Through Aligned Fiber Beds", *Polymer Engineering and Science*, Vol. 14, No. 6, June, 1974, pp.413-419.
2. Gutowski, T.G., et. al., "Consolidation Experiments for Laminate Composites", *Journal of Composite Materials*, Vol. 21, June, 1987, pp.650-669.
3. Lam, R.C. and Kardos, J.L., "The Permeability of Aligned and Cross-Plied Fiber Beds During Processing of Continuous Fiber Composites", Proceedings of American Society for Composites, Third Technical Conference, Seattle, Washington, September, 1988, pp.3-11.
4. Lam, R.C. and Kardos, J.L., "The Permeability and Compressibility of Aligned and Cross-Plied Carbon Fiber Beds During Processing of Composites", Proceedings of 47th Annual Technical Conference (ANTEC'89), SPE, New York, 1989, pp.1408-1412.
5. Skartsis, L. and Kardos, J.L., "The Newtonian Permeability and Consolidation of Oriented Carbon Fiber Beds", Proceedings of American Society for Composites, Fifth Technical Conference, E. Lansing, Michigan, June, 1990, pp.548-556.
6. Kim, Y.R., McCarthy, S.P., Fanucci, J.P., Nolet, S.C., and Koppernaes, C., "Resin Flow Through Fiber Reinforcements During Composite Processing", *SAMPE Quarterly*, April, 1991, pp.16-22.
7. Sangani, A.S. and Acrivos, A., "Slow Flow Past Periodic Arrays of Cylinders with Application to Heat Transfer", *International Journal of Multiphase Flow*, Vol. 8, No. 3, 1982, pp.193-206.
8. Berdichevsky, A.L. and Cai, Z., "Estimation of the Permeability of Aligned Fibers with the Self-Consistent Method and FE Simulation", accepted by *Polymer Composites*, 1992.
9. Scheidegger, A.E., The Physics of Flow Through Porous Media, University of Toronto Press, 1974, pp.75-78.
10. Kohnke, P.C., ANSYS Engineering Analysis System Theoretical Manual, Swanson Analysis Systems, Inc., 1989.
11. Fluid Dynamics International, FIDAP Theoretical Manual, 1990.
12. Adams, D.F. and Tsai, S.W., "The Influence of Random Filament Packing on the Transverse Stiffness of Unidirectional Composites", *Journal of Composite Materials*, Vol. 3, July, 1969, pp.368-381.
13. Cai, Z. and Berdichevsky, A.L., "An Improved Self-Consistent Method for Estimating the Permeability of a Fiber Assembly", accepted by *Polymer Composites*, 1992.

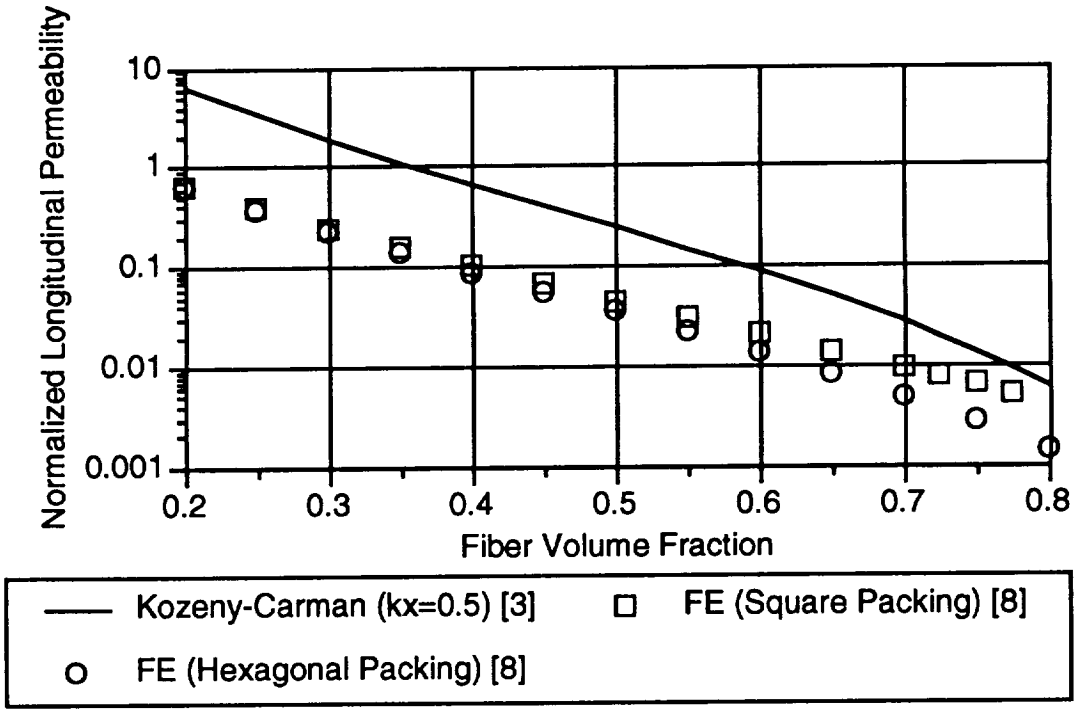

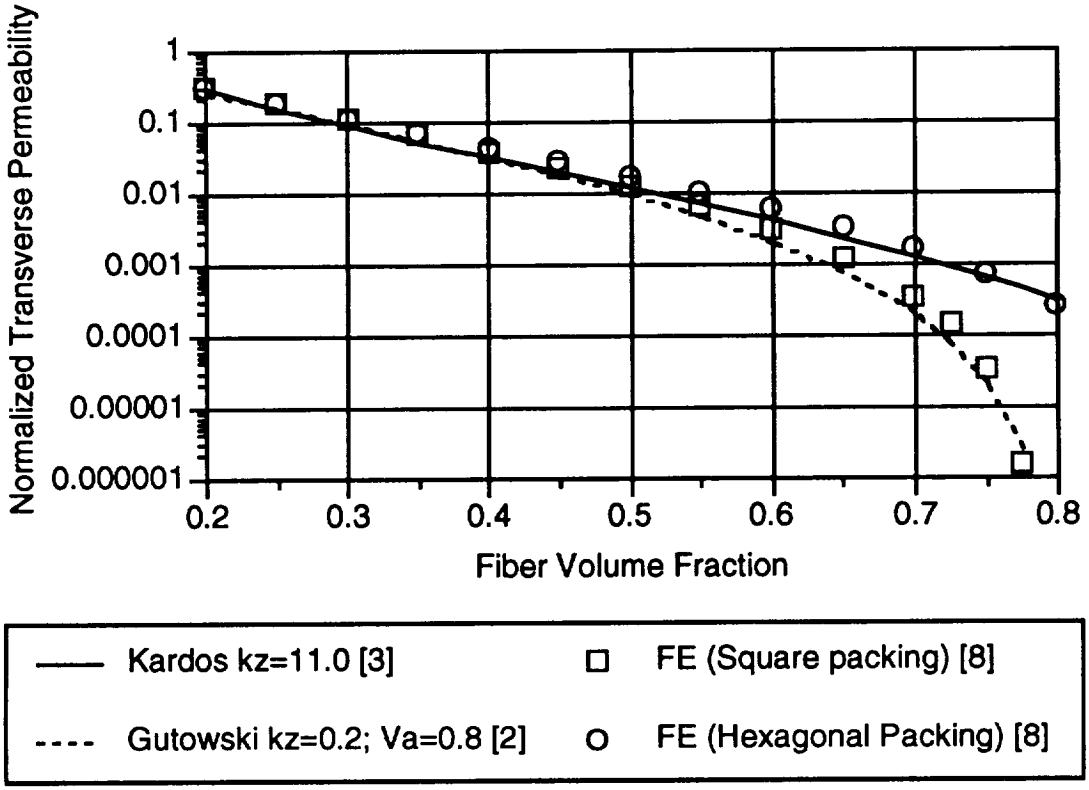

Fig. 1: Comparison of the permeability of idealized packing and other data.

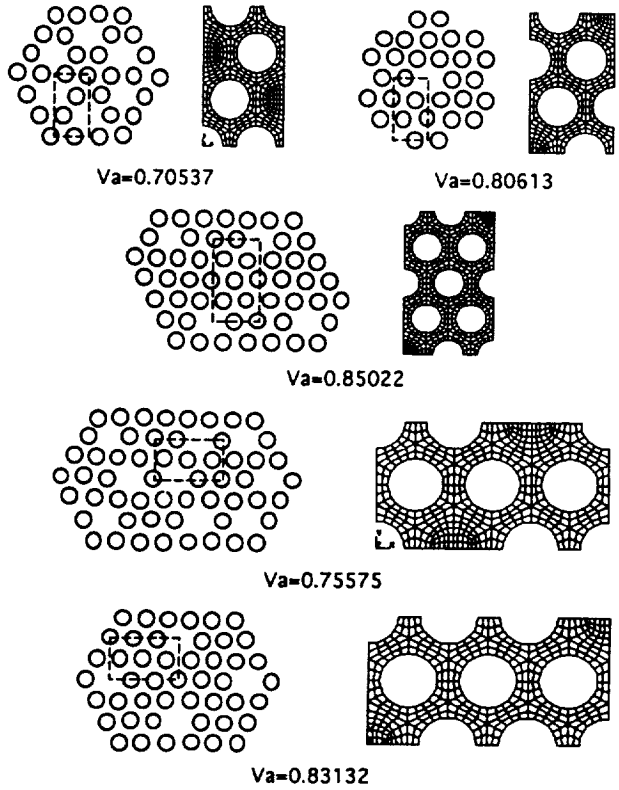

Fig. 2: Densely packed hollow hexagonal structures.

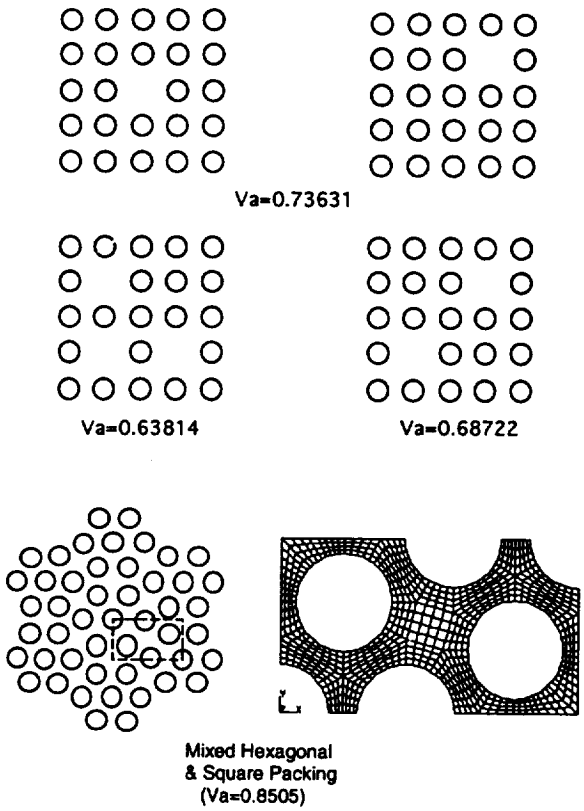

Fig. 3: Densely packed hollow square and mixed structures.

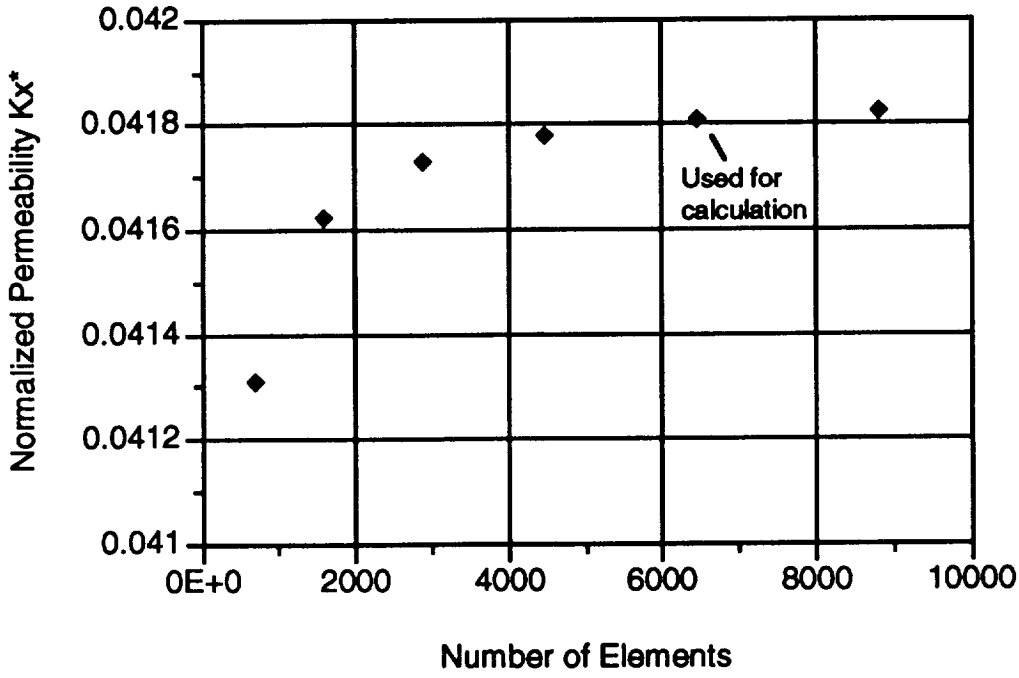

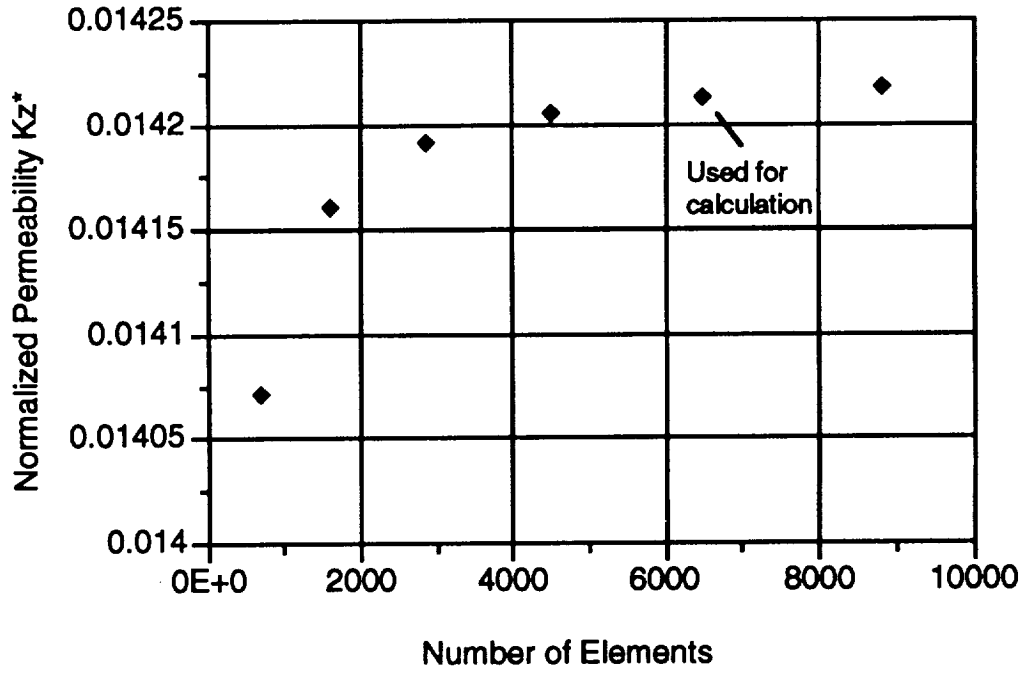

Fig. 4: Convergence of the numerical solution (with mixed packing model).

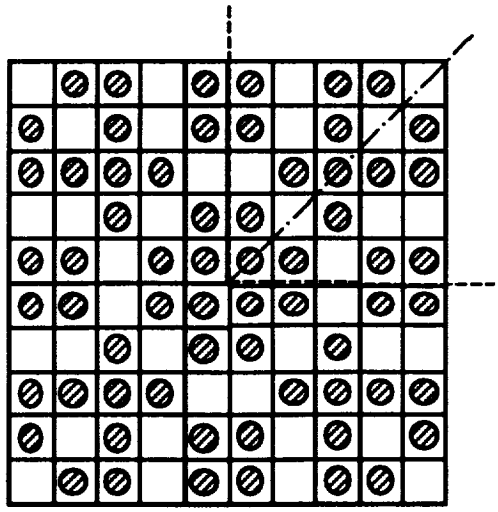

Computational Cell for "Random" Packing

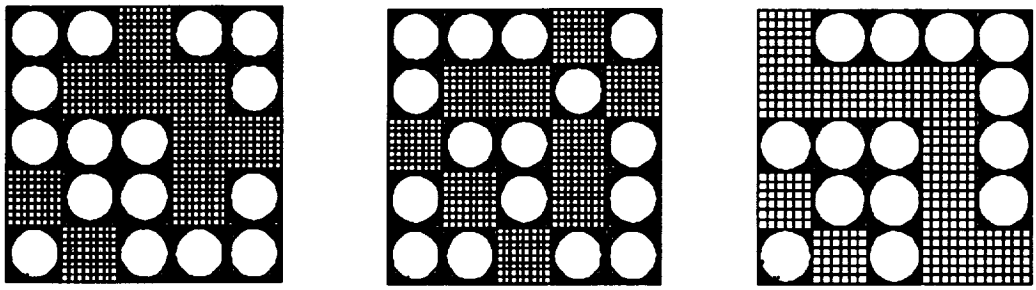

Randomly placed fibers

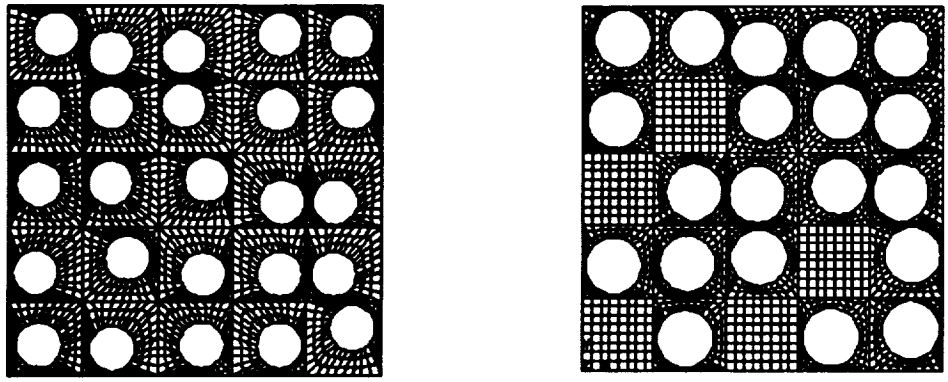

Fibers with random center positions

Fig. 5: Computational cell for "random" packing structures.

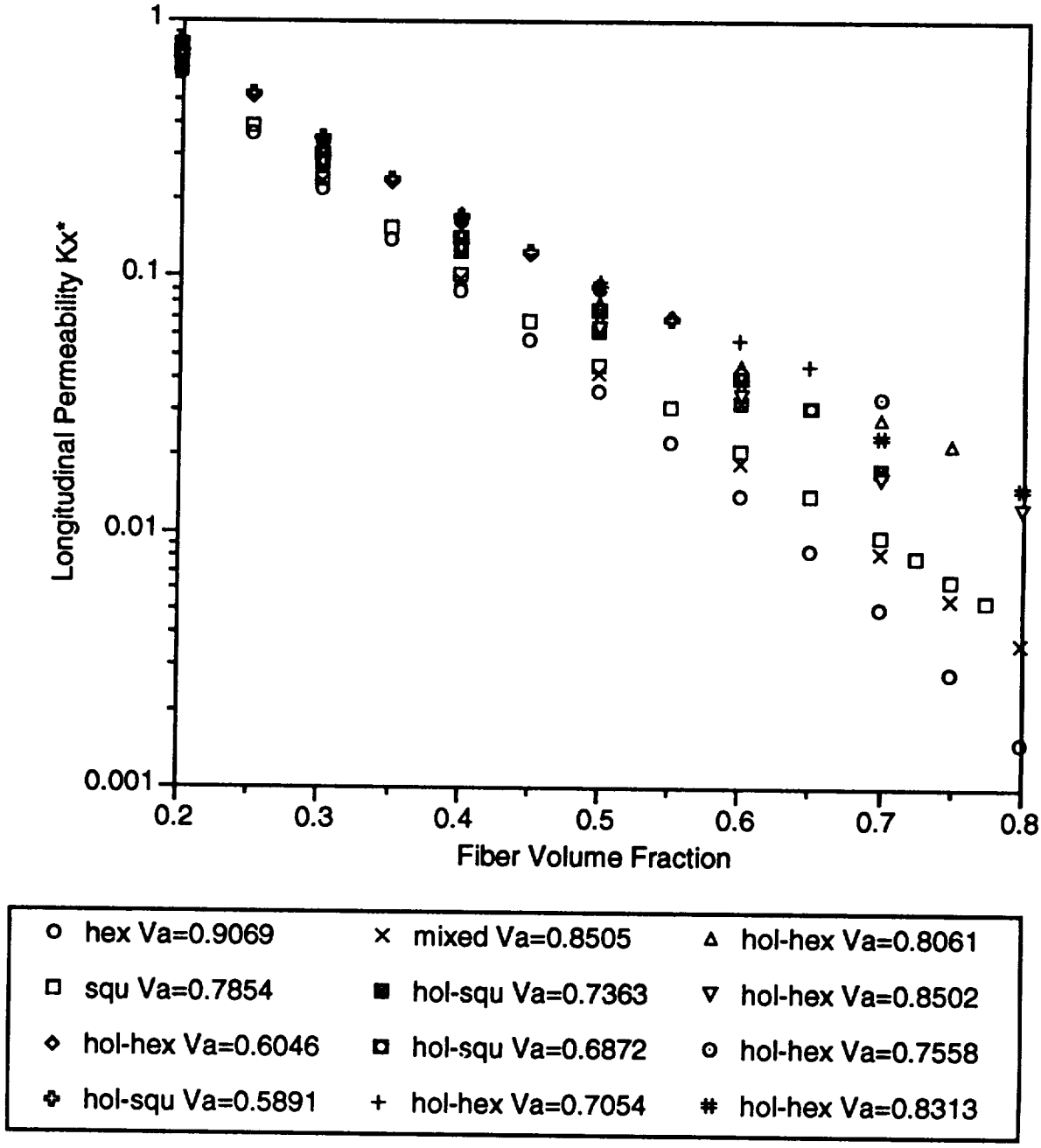

Fig. 6: Normalized longitudinal permeability comparison.

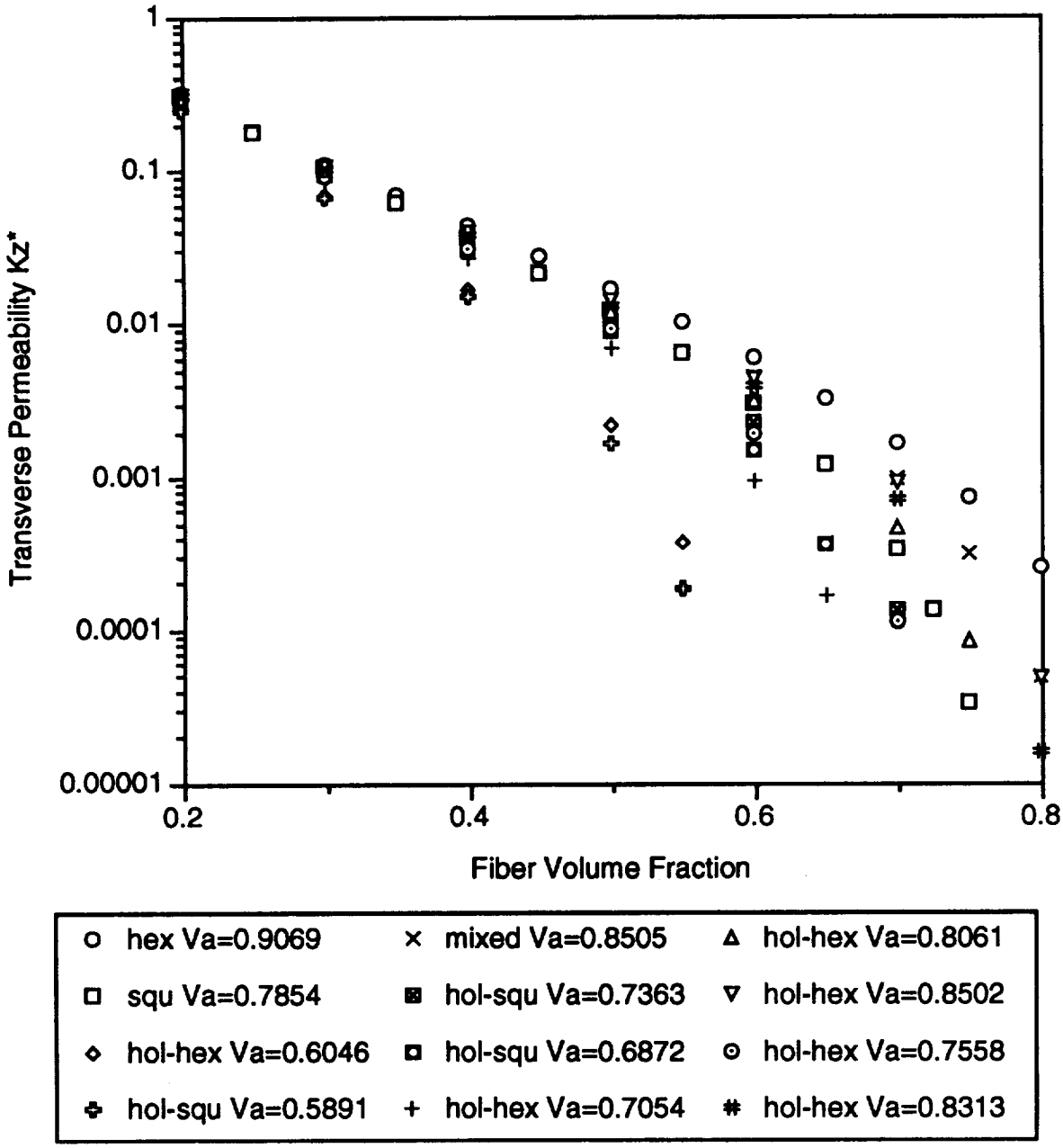

Fig. 7: Normalized transverse permeability comparison.

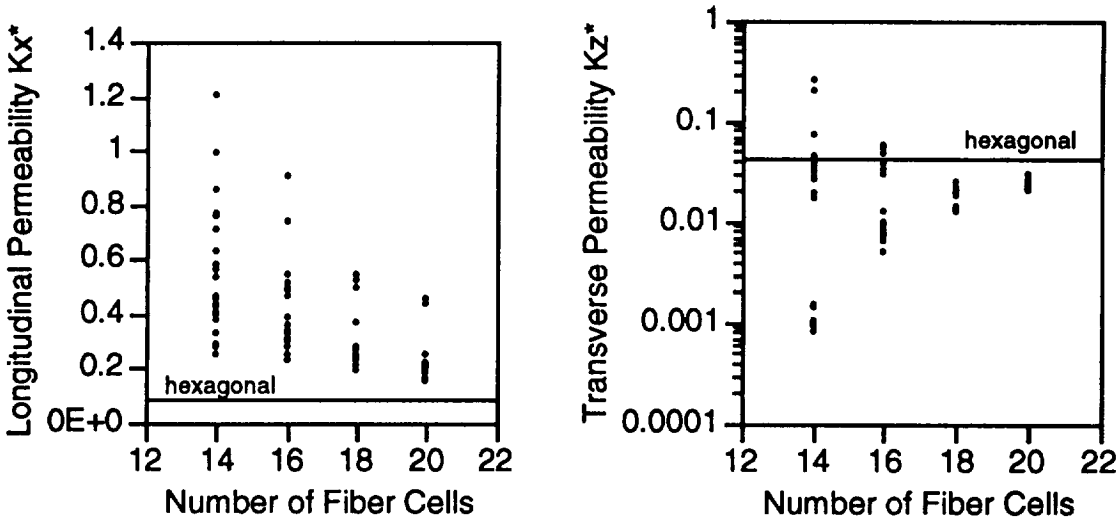

Fig. 8a: Permeability comparison with random model (V_f=0.4).

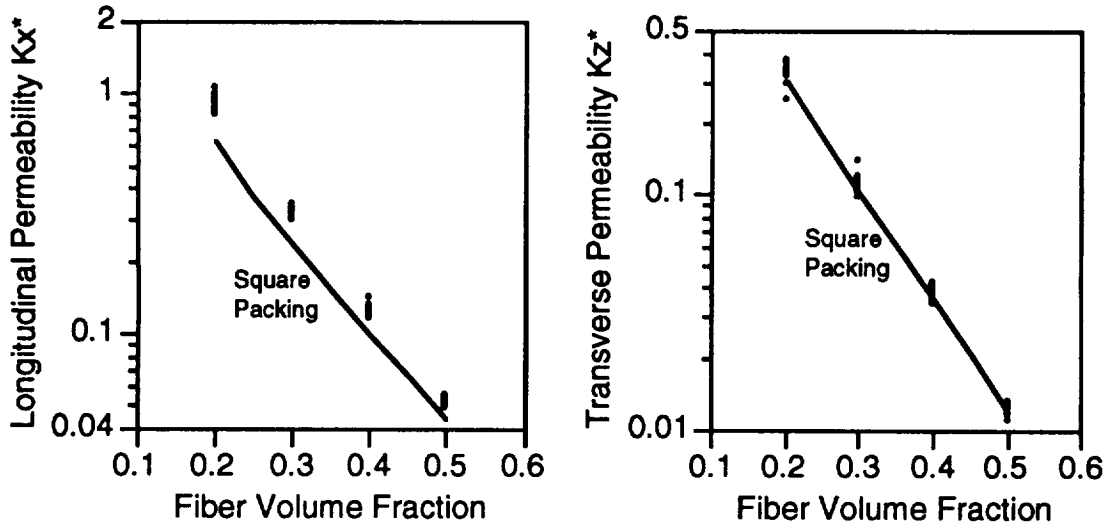

Fig. 8b: Permeability comparison of square packing with disturbances.

C-3